

REPORT DOCUMENTATION PAGE

Form Approved
OMB No. 0704-0188

Public reporting burden for this collection of information is estimated to average 1 hour per response, including the time for reviewing instructions, searching existing data sources, gathering and maintaining the data needed, and completing and reviewing this collection of information. Send comments regarding this burden estimate or any other aspect of this collection of information, including suggestions for reducing this burden to Department of Defense, Washington Headquarters Services, Directorate for Information Operations and Reports (0704-0188), 1215 Jefferson Davis Highway, Suite 1204, Arlington, VA 22202-4302. Respondents should be aware that notwithstanding any other provision of law, no person shall be subject to any penalty for failing to comply with a collection of information if it does not display a currently valid OMB control number. PLEASE DO NOT RETURN YOUR FORM TO THE ABOVE ADDRESS.

1. REPORT DATE (DD-MM-YYYY)		2. REPORT TYPE Technical Papers		3. DATES COVERED (From - To)	
4. TITLE AND SUBTITLE				5a. CONTRACT NUMBER N/A	
				5b. GRANT NUMBER	
				5c. PROGRAM ELEMENT NUMBER	
6. AUTHOR(S)				5d. PROJECT NUMBER 2308	
				5e. TASK NUMBER M19B	
				5f. WORK UNIT NUMBER	
7. PERFORMING ORGANIZATION NAME(S) AND ADDRESS(ES) Air Force Research Laboratory (AFMC) AFRL/PRS 5 Pollux Drive Edwards AFB CA 93524-7048				8. PERFORMING ORGANIZATION REPORT	
9. SPONSORING / MONITORING AGENCY NAME(S) AND ADDRESS(ES) Air Force Research Laboratory (AFMC) AFRL/PRS 5 Pollux Drive Edwards AFB CA 93524-7048				10. SPONSOR/MONITOR'S ACRONYM(S)	
				11. SPONSOR/MONITOR'S NUMBER(S)	
12. DISTRIBUTION / AVAILABILITY STATEMENT Approved for public release; distribution unlimited.					
13. SUPPLEMENTARY NOTES					
14. ABSTRACT					
15. SUBJECT TERMS					
16. SECURITY CLASSIFICATION OF:			17. LIMITATION OF ABSTRACT A	18. NUMBER OF PAGES	19a. NAME OF RESPONSIBLE PERSON Leilani Richardson
a. REPORT Unclassified	b. ABSTRACT Unclassified	c. THIS PAGE Unclassified			19b. TELEPHONE NUMBER (include area code) (661) 275-5015

Standard Form 298 (Rev. 8-98)
Prescribed by ANSI Std. Z39.18

21 separate items enclosed

103053

TP-1448-144

2309M19B
93 COMS

MEMORANDUM FOR PRS (Contractor Publication)

FROM: PROI (TI) (STINFO)

8 July 1998

SUBJECT: Authorization for Release of Technical Information, Control Number: **AFRL-PR-ED-TP-1998-144**
G. Vaghjiani (Raytheon STX), "Reaction Kinetics of $O(^3P)$ and OH with Diamine Rocket Fuels"
AIAA (Statement A)



AIAA-98-3542

**Reaction Kinetics of $O(^3P)$ and OH With Diamine
Rocket Fuels**

Ghanshyam L. Vaghjiani
Raytheon STX
Air Force Research Laboratory, AFRL/PRS
10 E Saturn Blvd
Edwards AFB, CA 93524
Tel: (805) 275 5657
Fax: (805) 275 6245
Email: ghanshyam_vaghjiani@ple.af.mil

20030103 053

**34th AIAA/ASME/SAE/ASEE
Joint Propulsion Conference & Exhibit
July 13-15, 1998 / Cleveland, OH**

REACTION KINETICS OF O(³P) AND OH WITH DIAMINE ROCKET FUELS

Ghanshyam L. Vaghjiani

Raytheon STX, Air Force Research Laboratory, AFRL/PRS, 10 E Saturn Blvd, Edwards AFB, CA 93524
Tel: (805) 275 5657, Fax: (805) 275 6245, Email: ghanshyam_vaghjiani@ple.af.mil

ABSTRACT

The gas phase kinetics of O(³P) and OH reactions with the three diamine fuels; N₂H₄, CH₃NHNH₂ and (CH₃)₂NNH₂ has been studied in a discharge flow-tube apparatus. The reactions were studied in 2 torr of He under pseudo-first-order conditions in the transient species concentration with a known excess of diamine concentration. The steady-state concentration temporal profiles of the transient species were directly monitored by fluorescence techniques to deduce the absolute second-order reaction rate coefficients. The Arrhenius expressions; $(7.35 \pm 2.16) \times 10^{-13} e^{(640 \pm 60)/T}$, $(2.71 \pm 0.04) \times 10^{-11} e^{-(190 \pm 50)/T}$ and $(1.96 \pm 0.29) \times 10^{-11} e^{(20 \pm 40)/T}$ cm³ molec⁻¹ s⁻¹ in the temperature range 252-640 K were obtained for reactions of O(³P) with N₂H₄, CH₃NHNH₂ and (CH₃)₂NNH₂, respectively. The corresponding expressions; $(1.25 \pm 0.19) \times 10^{-11} e^{(315 \pm 55)/T}$, $(2.88 \pm 0.04) \times 10^{-11} e^{(210 \pm 55)/T}$ and $(2.00 \pm 0.30) \times 10^{-11} e^{(330 \pm 80)/T}$ cm³ molec⁻¹ s⁻¹ in the range 232-374 K were determined for the OH reactions. Our recent measurement of the total yield of OH(X²Π) formation in the O + N₂H₄ reaction of (0.15 ± 0.05) at 298 K (of which ~ 50% was found to be produced hot with vibrational excitation up to the limit of reaction exothermicity) and the present observed experimental kinetic trends suggest that the initial addition of O(³P) and OH to the hydrazine molecule followed by rapid dissociation to products is an important process. Alkylation in the diamine molecule also allows direct H-abstraction mechanism to operate in these reaction systems.

INTRODUCTION

The reactions of atomic oxygen (O(³P)) and the hydroxyl radical (OH) with diamine fuels like hydrazine (N₂H₄), mono methyl hydrazine (CH₃NHNH₂) and unsymmetrical dimethyl hydrazine ((CH₃)₂NNH₂) are important elementary processes during combustion in bi-propellant (diamine/nitrogen tetroxide (N₂O₄)) rocket motors such as those in the Titan launch vehicles. Also, numerous spacecraft that operate in low earth orbit (LEO), ~ 180 km and above, use N₂H₄ in attitude-control jets and its mono-methylated analogue as a fuel in thruster engines such as those on the Space Shuttle. Although most of the fuel is consumed in the rocket chamber, some escapes in the unburned state especially at engine shut down.

Since the ambient atmosphere at LEO altitudes consists mainly of atomic oxygen, the ejected fuel fragments are thought to degrade primarily via the O(³P) reaction. Even though molecular band emissions in the uv (and visible) have been observed in O-atom/diamine rocket plumes and flames,¹⁻⁵ the understanding of the chemical pathways involved is far from complete. Competition between pyrolysis and initial oxidation of the fuel needs to be understood to establish the mixing ratio of the exhaust effluents. The products of these processes themselves undergo further oxidation reactions of which some may directly produce the excited state species in chemiluminescent reactions, or produce metastable precursors. These precursors can then transfer their electronic energy to the surrounding ground state species. The quantum yields for uv/visible radiation from these excited species will depend on their radiative and reactive lifetimes. The latter being determined by both physical quenching and chemical transformations. One also needs to consider the possible effect of the relative velocity between the

Copyright © 1998 by Ghanshyam L. Vaghjiani,
Published by the American Institute of Aeronautics and
Astronautics, Inc. with permission.

exhaust fragments and the ambient O-atoms for any given oxidation reaction considered. The relative velocity can range from the sum of the LEO velocity (typically $\sim 7.8 \text{ km s}^{-1}$) and the exhaust plume velocity (typically $\sim 3.5 \text{ km s}^{-1}$) to the difference in the two values depending on the direction of the rocket firing. The role of ionized chemical species and of O_2 in the plume/thermosphere must also be investigated. Only when the interplay between the various processes described above is properly understood can we hope to make reliable predictions/assessments of uv/visible-plume signatures, and other spacecraft-plume effects such as the Shuttle Glow, and the contamination of spacecraft surfaces or onboard instrumentation.

Since the initial thermospheric oxidation reactions of the exhaust effluents will determine the way in which the subsequent plume chemistry unfolds, we have chosen in this work to investigate and properly characterize the reaction chemistry of the diamine fuel plus O-atom interactions under laboratory conditions. In the very near future, we shall report on the O-atom and O_2 oxidation chemistry of several different pyrolyzed fuel fragments found in diamine exhaust plumes.

Also, hydrazine fuels can be released into the lower atmosphere as a result of inadvertent spills of propellants or due to a launch abort. Monitoring the atmospheric concentrations of these species both in the gas phase and in aerosols, and modeling their transport and chemical transformations are essential to the evaluation of their environmental human health impact and launch constraint scenarios. The two main tropospheric oxidants for these fuels are expected to be OH and O_3 . Here we also report the gas phase kinetics of OH reactions.

EXPERIMENTAL TECHNIQUE

The discharge flow-tube apparatus employed in this work has previously been described in detail elsewhere.⁶ A schematic of the apparatus is shown in Fig. 1. Here we only provide details of the experimental procedures employed to determine the reaction rate coefficient data. A small sample of liquid diamine was vaporized using He and carried into an absorption cell for 213.9-nm photometric determination of its gas phase concentration before sending the mixture for further dilution via a sliding injector into the flow-tube carrying an excess flow of He. The uv-absorption cross sections of $\sigma_{213.9} = 220.5 \times 10^{-20}$,

248.9×10^{-20} and $399.9 \times 10^{-20} \text{ cm}^2 \text{ molec}^{-1}$, respectively for N_2H_4 , CH_3NHNH_2 and $(\text{CH}_3)_2\text{NNH}_2$ were used.^{7,8} A fixed side-arm microwave discharge port was used to introduce the $\text{O}(^3\text{P})$ or OH into flow-tube. $\text{O}(^3\text{P})$ was made either from the discharge of a 1% mixture of O_2 in He or pure N_2 . In the latter case, the N-atoms produced were titrated in a flow of 1% mixture of nitric oxide in He. The titration reaction, $\text{N} + \text{NO} \rightarrow \text{O} + \text{N}_2$, was followed to the end-point photometrically by monitoring the NO_2^* emission produced in the accompanying reaction, $\text{O} + \text{NO} \rightarrow \text{NO}_2^*$. OH was made from the discharge of a 1% mixture of H_2 in He to produce H-atoms, followed by the quantitative titration, $\text{H} + \text{NO}_2 \rightarrow \text{OH} + \text{NO}$, or from the discharge of a 1% mixture of CF_4 in He to make F-atoms, followed by the reaction, $\text{F} + \text{H}_2\text{O} \rightarrow \text{OH} + \text{HF}$. The number density of the diamine in the reaction zone of the flow-tube was always in an excess of the initial radical number density, by 50-1000 times, and calculated from the known flow rates used to carry out the dilution, and the measured pressure and temperature of the reaction zone and the absorption cell. The capacitance manometers, the chromel-alumel thermocouples and the electronic mass flow meters used to flow the gases had previously been calibrated.

The reaction zone temperature in the experiments was varied in the range 232-640 K and the flow-tube operated at a pressure of 2 torr of He (a few experiments were done at 8 torr). Typical linear gas velocity, v , of 1800-3500 cm s^{-1} of He flow was maintained in the 1-inch-diameter flow-tube. The plug-flow conditions^{9,10} thus established in the flow-tube allowed us to follow the reaction kinetics of the [radical] in a known excess of [diamine] under pseudo-first-order conditions. Typical initial radical concentration was in the range $(1-5) \times 10^{10} \text{ molec cm}^{-3}$. The steady-state [radical] was monitored as a function of the reaction distance, z , between the point of reagent mixing at the injector tip and the fixed detection zone downstream of the flow-tube. The $\text{O}(^3\text{P})$ was excited at 130.2-130.6 nm using a microwave discharge lamp and monitored orthogonally to it by cw-resonance fluorescence detection using photon-counting techniques.^{6,11,12} The OH was probed using a tunable pulsed laser operating at $\sim 282.15 \text{ nm}$ to excite the Q₁₂ line of the OH transition, ($\text{A}^2\Sigma^+, v' = 1 \leftarrow \text{X}^2\Pi, v'' = 0$). The resulting laser-induced fluorescence due to the transitions, ($\text{A}^2\Sigma^+, v' = 1 \rightarrow \text{X}^2\Pi, v'' = 1$, bandhead at 312.16 nm) and ($\text{A}^2\Sigma^+$,

$v' = 0 \rightarrow X^2\Pi$, $v'' = 0$, bandhead at 306.36 nm), ensuing from the detection zone was detected orthogonally to the laser beam by gated-charge integration/signal averaging techniques.^{6,13} The inner walls of the flow-tube were suitably coated to minimize radical loss rates at the surfaces. Most of the O-atom work was carried out in a resistively heated quartz flow-tube that had been cleaned in a 30% H_3PO_4 solution, while all OH (and some O-atom) work was done in a halocarbon coated Pyrex flow-tube with an outer Pyrex heating jacket. No systematic dependence of the measured reaction rate coefficient was observed on switching the movable diamine inlet to a fixed side-arm inlet and the fixed radical inlet to a suitable sliding source.

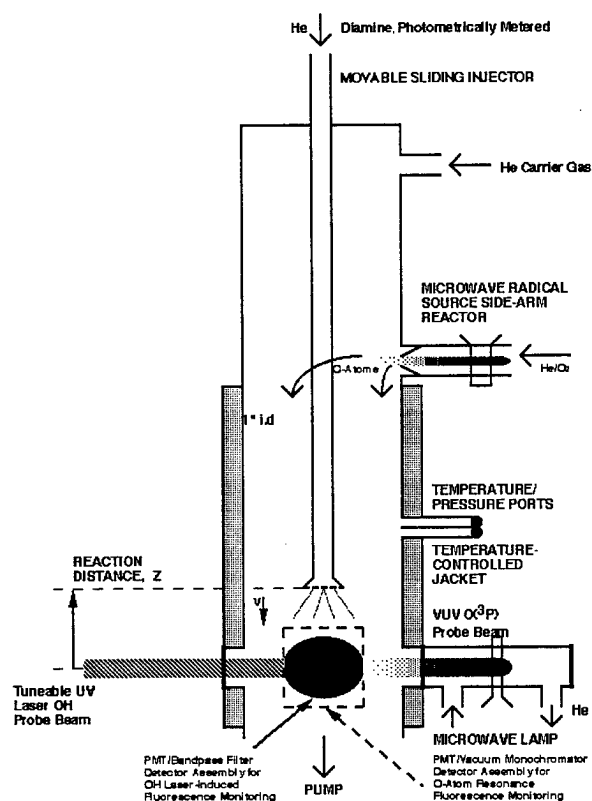


FIG. 1. Schematic of one version of the discharge flow-tube apparatus employed in this work.

Materials

He (>99.9997%) carrier gas from U. S. Bureau of Mines and N_2 (99.9995%) from Spectra Gases were used as received. Hydrocarbon-free N_2H_4 (Viking

Grade) from Edwards AFB, $(CH_3)_2NNH_2$ (>99.3%) and CH_3NHNH_2 (>99.5%) from Olin Chemicals were subjected to several freeze-thaw purification cycles at a grease-less vacuum line, and the purified distillates dried over BaO or CaH_2 . NO (99.0%) supplied by Matheson Gas Products was passed slowly through a trap containing silica gel at 173 K to remove most of the NO_2 and N_2O impurities and then frozen in a second trap over silica gel maintained at 77 K. The condensate was subjected to thorough pumping. NO was taken out from this trap as it warmed up slightly above 77 K and transferred into a 12- \angle Pyrex bulb where it was diluted with He to make up a standard 1% NO in He titration mixture. NO_2 (99.9%) from M. G. Scientific Gases was mixed with excess O_2 to react away any NO present and the mixture collected in a trap over silica gel at 213 K. The excess O_2 and any other volatiles were pumped off and the condensate subjected to several freeze-thaw purification cycles. A standard 1% NO_2 in He titration mixture was prepared. O_2 (99.991%) from Big Three Industries, CF_4 (99.7%) from Scott Specialty Gases and H_2 (99.999%) from Linde Specialty Gases were used as supplied to make up 1% mixtures in He. The water was distilled in the laboratory.

RESULTS

Since the [diamine] is always in a great excess over the [OH] in the flow-tube, it can be shown that the observed pseudo-first-order decay coefficient, k , for OH is given by, $\ln\{OHS/OHS_0\} = -k.t$. Where OHS is the net (background-subtracted) OH laser-induced fluorescence signal strength recorded at the detection zone for a reaction time of $t = z/v$. The flow-tube reaction distance, z , is defined to be the length between the tip of the injector where the diamine enters and the OH fluorescence detection axis. v is the bulk linear flow velocity of the He carrier gas. OHS_0 is the signal strength that would be observed for $z = 0$ and corresponds to the initial concentration, $[OH]_0$, available at the detection zone when OH is introduced from the fixed side-arm reactor upstream of the flow-tube. (Note that a constant fraction of OH is lost to the flow-tube walls from the point where it enters and the point where it is detected. This loss term rate, $k_{w,OH}$, does not affect the above kinetic analysis, however, we have minimized it by coating the tube walls with thin films as described earlier, so as to maximize the observed signal-to-noise ratio. A similar analysis can be written for the $O(^3P)$ reactant.

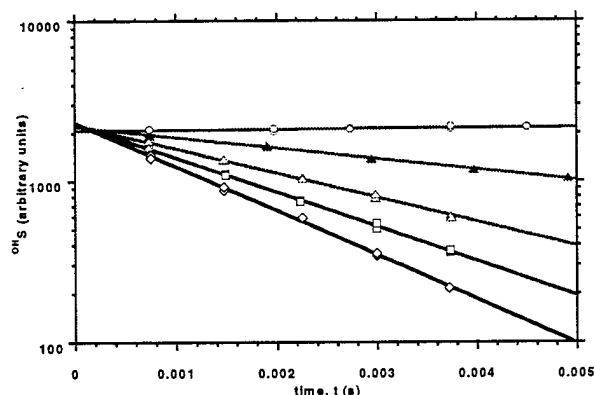


FIG. 2. Measured temporal profiles of OH signal, OH_S , in different $[(\text{CH}_3)_2\text{NNH}_2] = 0$ (open circles), $= 0.292 \times 10^{13}$ (solid triangles), $= 0.643 \times 10^{13}$ (open triangles), $= 0.957 \times 10^{13}$ (open squares), and $= 1.339 \times 10^{13}$ molec cm^{-3} (open diamonds) at 373 K and in 2 torr He.

Fig. 2 shows typical plots of the determined OH_S signal on a logarithmic scale as a function of reaction time, t . The data points are the mean OH signals observed by averaging 100 fluorescence pulses. (Note that the time axis need not be absolute provided we accurately know the relative time increments (i.e. Δz) between the data points. The precision of z measurements is known to be very high (to within ± 0.05 cm) in our experiments.) The solid lines are exponential fits to the data points whose slopes yield values for the observed pseudo-first-order decay coefficients, k . The positive slope (open circles) obtained in the absence of $(\text{CH}_3)_2\text{NNH}_2$ is consistent with the loss of OH on the injector walls. As the injector is pulled back, less of its wall is exposed to the radical flow, and the OH signal increases. Typically this loss term, k_{in} , was measured to be ~ 10 – 20 s^{-1} , and was used to correct k to arrive at the net loss rate decay coefficient, k_{net} . Correction of k_{net} for axial diffusion^{9,10} using, $k_{\text{corr}} = k_{\text{net}}(1 + k_{\text{net}}\mathcal{D}/v^2)$, where \mathcal{D} , in units of $\text{cm}^2 \text{s}^{-1}$, is the diffusion coefficient of OH in He, resulted in $\leq 5.5\%$ upward correction to the k_{net} values.¹⁴ The absolute second-order rate coefficient for the reaction, $\text{OH} + (\text{CH}_3)_2\text{NNH}_2 \rightarrow$ products, was determined from the slope of a plot of k_{corr} versus $[(\text{CH}_3)_2\text{NNH}_2]$ employed. Fig. 3 shows a

typical plot at 373 K with the linear-least-squares fit to the data points. Fig. 4 shows the observed temperature dependencies of the absolute second-order rate coefficients for the OH reactions with the three diamines studied here. The corresponding temperature dependencies of the $\text{O}(^3\text{P})$ reactions are shown in Fig. 5.

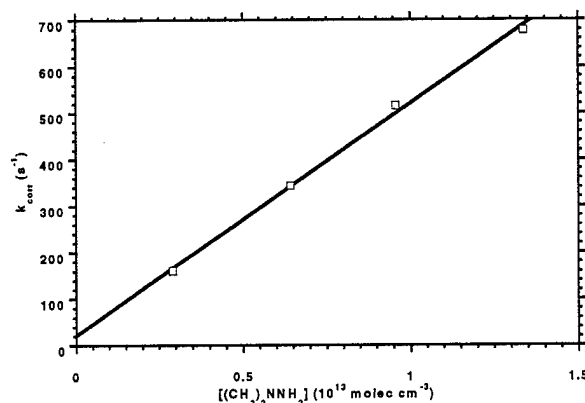


FIG. 3. Plot of corrected pseudo-first-order decay coefficients, k_{corr} , versus the $[(\text{CH}_3)_2\text{NNH}_2]$ of Fig. 2. The absolute second-order rate coefficient is $(4.98 \pm 0.75) \times 10^{-11} \text{ cm}^3 \text{ molec}^{-1} \text{ s}^{-1}$ at 373 K.

DISCUSSION

OH Reactions

The reactions of OH with the diamines are very fast, close to the gas-kinetic limit, and show slight negative temperature dependencies. The Arrhenius fits to the data points of Fig. 4 give the following expressions; $(1.25 \pm 0.19) \times 10^{-11} e^{(315 \pm 55)/T}$, $(2.88 \pm 0.04) \times 10^{-11} e^{(210 \pm 55)/T}$ and $(2.00 \pm 0.30) \times 10^{-11} e^{(330 \pm 80)/T} \text{ cm}^3 \text{ molec}^{-1} \text{ s}^{-1}$, in the temperature range 232–374 K, for reactions with N_2H_4 , CH_3NHNH_2 and $(\text{CH}_3)_2\text{NNH}_2$, respectively. Also, there is generally an increase in the OH reactivity along the above homologous series. Previous flash photolysis-resonance fluorescence study of Harris et al.¹⁵ reported a weaker temperature dependence of $4.4 \times 10^{-11} e^{(116 \pm 176)/T} \text{ cm}^3 \text{ molec}^{-1} \text{ s}^{-1}$, in the range 298–424 K, for the $\text{OH} + \text{N}_2\text{H}_4$ reaction. No dependence was observed on the Ar pressure which was varied in the range 25–50 torr. Also under these conditions, a temperature independent rate coefficient

of $(6.5 \pm 1.3) \times 10^{-11} \text{ cm}^3 \text{ molec}^{-1} \text{ s}^{-1}$ was reported for the $\text{OH} + \text{CH}_3\text{NHNH}_2$ reaction. However, for the $\text{OH} + (\text{CH}_3)_2\text{NNH}_2$ reaction, they could only estimate a room temperature value of $(5 \pm 2) \times 10^{-11} \text{ cm}^3 \text{ molec}^{-1} \text{ s}^{-1}$ because of severe handling problems encountered with this dialkylated diamine. At 298 K, Harris et al.'s values are $\sim 80\%$ larger, $\sim 11\%$ larger and $\sim 17\%$ smaller than our values for N_2H_4 , CH_3NHNH_2 and $(\text{CH}_3)_2\text{NNH}_2$, respectively. An earlier communication from Hack et al.¹⁶ for the $\text{OH} + \text{N}_2\text{H}_4$ reaction studied by discharge flow-tube-ESR technique reported a value of $2.2 \times 10^{-11} \text{ cm}^3 \text{ molec}^{-1} \text{ s}^{-1}$ at 298 K which is $\sim 39\%$ smaller than our value.

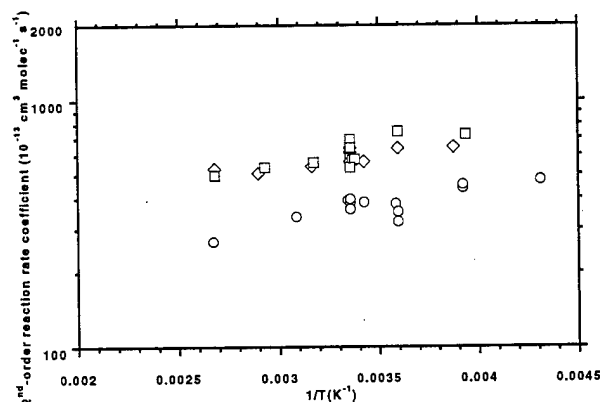


FIG. 4. The temperature dependencies of the absolute second-order rate coefficients for OH reactions with, N_2H_4 (open circles), CH_3NHNH_2 (open diamonds), and $(\text{CH}_3)_2\text{NNH}_2$ (open squares).

The lack of proper quantification of the diamine number density in the previous studies might possibly be one of the reasons as to why there is disagreement in the absolute values of some of the rate coefficients. We have made accurate, to within $\pm \sim 6\%$,⁷ in-situ measurements of the [diamine] in our experiments and have confirmed that the measured rate coefficients are independent of the $[\text{OH}]_0$ range employed. The overall accuracy of the rate coefficients in this work is expected to be in the range $\pm (15-18)\%$ (precision plus systematic errors included).⁶ Some problematic wall effects were noticed when using $(\text{CH}_3)_2\text{NNH}_2$, especially at temperatures below 253 K. The flow-tube became easily contaminated with yellow oily deposits on prolonged exposures which resulted in unusually large OH wall loss rates compared to that

observed in a freshly coated flow-tube with the halocarbon wax. This was evident from the larger than normal intercepts in k_{corr} versus $[(\text{CH}_3)_2\text{NNH}_2]$ plots even at the lowest $[\text{OH}]_0$ used. The flow-tube was frequently re-waxed to minimize this problem. Data above 374 K could not be obtained in this flow-tube because of fogging of the optical windows due to condensation of the wax vapor which resulted in a dramatic fall in the signal-to-noise ratio of the fluorescence signal. The quartz flow-tube showed enhanced wall loss rates of OH in the presence of the diamine and was therefore not used. We shall report on the rate coefficients at temperatures, $T > 374 \text{ K}$ in the near future using a resistively heated pulsed photolysis reactor.¹⁷

The magnitude and the weak temperature and lack of pressure effects of the $\text{OH} + \text{N}_2\text{H}_4$ reaction rate coefficient suggests that the simple direct metathesis of H-atom may not be important compared to addition of the OH followed by dissociation of the intermediate into products. The findings of a recent ab initio study by Armstrong et al.¹⁸ on this reaction are qualitatively consistent with the present experimental observations. The shape of the potential energy profile along the reaction coordinate leading to $\text{N}_2\text{H}_3 + \text{H}_2\text{O}$ as the products was examined. At the B3LYP/6-31+G(D, P) level, a single pre-reaction complex was found characterized by an OH--NN hydrogen bond (OH--N distance 1.859 Å, H--N--N angle 170.1°). The G2(MP2) energy of this was lower by $\sim 5.5 \text{ kcal mol}^{-1}$ than that of $(\text{N}_2\text{H}_4 + \text{OH})$. Also, MP2 optimization with the same basis set yielded essentially the same structure for the complex. However, no transition-state for the direct H-abstraction by OH could be located at the B3LYP/6-31+G(D, P) level. Any approach by OH to an endo-H of hydrazine resulted in H-atom loss without activation. Instead, a transition-state structure for inversion of the N-atom bearing a hydrogen in close proximity to the hydroxyl was located at this level (N--H--OH angle 120.7°, NH--OH distance 1.707 Å). The normal mode with the imaginary frequency suggested that N-inversion would be accompanied by H-atom loss since the separation between the H and O was decreased, while the N--H distance remained the same. The G2(MP2) energy of this transition-state was $\sim 2.7 \text{ kcal mol}^{-1}$ above that of the separated reactants. By contrast, at MP2/6-31+G(D, P) level, a well defined transition-state structure for H abstraction by OH was found. This transition-state was directly connected to the hydrogen-bonded pre-reaction complex, with the G2(MP2) energy being $\sim 1.3 \text{ kcal mol}^{-1}$ lower than that

of the reactants. Also, single-point QCISD(T)/6-31+G(D, P) calculations along the MP2 intrinsic reaction coordinate further confirmed the existence of an early transition-state well above the initial pre-reaction complex but below the separated reactants (the NN-H bond being broken was elongated by only ~ 7% while the H-OH bond forming had already reached a length that was ~ 1.5 times that of the final separation in the water molecule). Such a description of the energetics of the reaction intermediaries would predict a negative experimental activation energy and a pressure insensitive rate coefficient.¹⁹ It would be most interesting to see how the computed barrier to H-abstraction and vibrational frequency information on the transition-state and pre-reaction complex predict the absolute magnitude and temperature dependence of the OH + N₂H₄ reaction rate coefficient by means of transition-state theory rate expressions.

The introduction of the CH₃ moiety in the hydrazine molecule opens up the possibility of direct H-abstraction from the stronger C-H bonds, or enhancement of hydrogen bonding tendency and eventual removal of the H-atom from the weak N-H bond which weakens even further due to the electron-donating effect of the methyl group. On the other hand, fewer N-H sites (but more C-H sites) are present on increased methylation. Experimentally, we see an increase in the measured rate coefficient for CH₃NHNH₂ and much less thereafter for (CH₃)₂NNH₂. Deuterium isotopic studies on the reaction rates and product yields will further help clarify the nature of the reaction mechanism in these systems.

Using an average [OH] of 5×10^6 molec cm⁻³ and a standard mean temperature of 279 K for the lower atmosphere, we calculate the lifetimes to be ~ 1.5, ~ 0.9 and ~ 0.9 hr, respectively for the oxidation of N₂H₄, CH₃NHNH₂ and (CH₃)₂NNH₂ by the hydroxyl radical. Ozone is also thought to react rapidly with these diamines.²⁰ However, the absolute rate coefficients for these reactions have not been measured. Proper atmospheric chemical lifetimes of these diamines will be calculable when this data becomes available.¹⁷ This will allow reliable assessments to be made on the urban impact of the inherent toxicity and carcinogenic potency of the diamines (and their oxidation products such as dimethylnitrosamine from the (CH₃)₂NNH₂ + O₃ reaction) when they are accidentally released at vehicle launch pads or at fill stations.

O(³P) Reactions

Compared to OH, the O(³P) atom is less reactive towards the three diamines. However, the reactions are still fast and show weak temperature dependencies. The Arrhenius fits to the data points of Fig. 5 give the absolute second-order rate coefficient expressions; $(7.35 \pm 2.16) \times 10^{-13} e^{(640 \pm 60)/T}$, $(2.71 \pm 0.04) \times 10^{-11} e^{-(190 \pm 50)/T}$ and $(1.96 \pm 0.29) \times 10^{-11} e^{(20 \pm 40)/T}$ cm³ molec⁻¹ s⁻¹, in the temperature range 252-640 K and in 2 torr of He, for reactions with N₂H₄, CH₃NHNH₂ and (CH₃)₂NNH₂, respectively. Again, an increase in the rate coefficient is observed along the indicated homologous series. For O + N₂H₄, Gehring and co-workers²¹ reported much larger rate coefficients with a positive temperature dependence of $1.4 \times 10^{-10} e^{(-604/T)}$ cm³ molec⁻¹ s⁻¹, in the temperature range 243-463 K and in 2.7 torr of Ar pressure. They used an excess of [O(³P)] and mass-spectrometrically monitored [N₂H₄] decays in their discharge flow-tube system. Incorrect calibration of the [O(³P)] and the presence of other much more reactive species could result in apparently enhanced [N₂H₄] decays with a positive temperature dependence for the measured rate coefficient. Lang²² used a photolytic method to produce O-atoms in an excess of [diamine] and monitored the [O(³P)] decay by cw-resonance fluorescence in 1-50 torr of N₂ pressure. No pressure dependence of the rate coefficient was seen. The values at 296 K are higher than our measured values by ~ 55%, ~ 12%, and ~ 10%, respectively for N₂H₄, CH₃NHNH₂ and (CH₃)₂NNH₂. The presence of unknown reactive impurities in Lang's sample of N₂H₄ would result in an apparently larger second-order rate coefficient. In light of the good agreement for the values of CH₃NHNH₂ and (CH₃)₂NNH₂, this problem doesn't seem to be significant in the alkylated samples.

Checks were performed to show that our measured rate coefficients were independent of the He pressure (up to 8 torr) or the [O(³P)]₀ range employed ($(0.1-20) \times 10^{11}$ molec cm⁻³). Above ~ 640 K, slight charring in the quartz flow-tube was seen, indicating that thermal decomposition of the alkylated diamines was occurring. Below ~ 252 K, the waxed flow-tube required frequent cleaning to remove the oily deposits from prolonged exposure to the diamine flow. Thus rate data beyond these temperature limits was not collected.

In our previous work,⁶ we showed that the $O + N_2H_4$ reaction proceeded $\sim 15\%$ of the time via single-H-abstraction to give OH as the product ($\sim 50\%$ of which is produced vibrationally hot). Other earlier work has shown that the preferred reaction channel is the elimination of H_2O in a direct reaction via a cyclic-transition-state involving the HN-NH system.^{21,23} As the OH can form from 4 similar N-H sites and the H_2O only from 2 distinct HN-NH approaches, the per site O-atom rate coefficient for OH and H_2O production in N_2H_4 is calculated to be 2.36×10^{-13} and $26.8 \times 10^{-13} \text{ cm}^3 \text{ s}^{-1}$, respectively. Since the H_2O formation channel should not be possible in $(CH_3)_2NNH_2$, and assuming no change in the N-H bond reactivity, the per CH_3 group rate coefficient for (the only remaining) H-abstraction channel by the O-atom is then calculated to be $103 \times 10^{-13} \text{ cm}^3 \text{ s}^{-1}$. This would then predict a total CH_3NHNH_2 rate coefficient of $135 \times 10^{-13} \text{ cm}^3 \text{ molec}^{-1} \text{ s}^{-1}$, which compares well with our value of $143 \times 10^{-13} \text{ cm}^3 \text{ molec}^{-1} \text{ s}^{-1}$ of Fig. 5. Also, if the assumptions of the reaction mechanism we have made are correct we should observe an OH yield of close to unity in the $O + (CH_3)_2NNH_2$ reaction and $\sim 80\%$ in the corresponding CH_3NHNH_2 reaction. These OH yield measurements are currently in progress. Excitation of OH vibrations in these reactions has also been seen.¹⁷

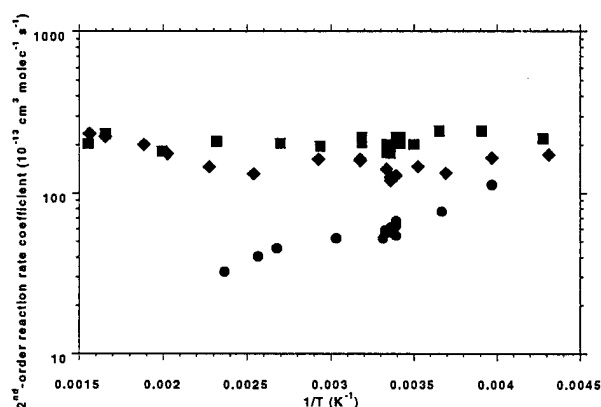


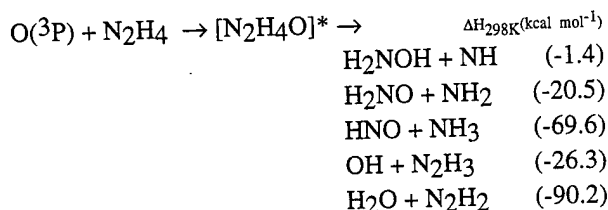
FIG. 5. The temperature dependencies of the absolute second-order rate coefficients for $O(^3P)$ reactions with, N_2H_4 (solid circles), CH_3NHNH_2 (solid diamonds), and $(CH_3)_2NNH_2$ (solid squares).

However, the good agreement between the observed rate coefficients and the above analysis might just be fortuitous, since there is some evidence in the literature that the N-H bond strength might be varying in the alkylated diamines.²³⁻²⁶ We might then expect a trend in the reaction rate at the N-H sites as well as at the C-H sites of the methyl moiety, where reactivity of the C-H bond might also vary depending on the degree of methylation at the N-center. Precise conclusions as to which of the two effects is more important can not yet be drawn. Studies using D-substituted diamine analogs where kinetic isotope effects are measured, and product identities and absolute branching yields are determined should help clarify the situation.

It is encouraging to know that in the related amine homologous series: NH_3 , NH_2CH_3 , $NH(CH_3)_2$ and $N(CH_3)_3$, a similar trend for reaction with O-atoms is observed.^{27,28} The 298 K reaction rate coefficient increases with increasing methylation, indicating perhaps increased importance of reaction at the C-H site. Though, it must also be noted that both the N-H and C-H bond strengths decrease with increased methylation in this amine series.²⁹ For OH reactions, the reactivity trend is: $NH_3 < NH_2CH_3 < N(CH_3)_3 < NH(CH_3)_2$, thus showing here, that where possible, the N-H site competes with the C-H site.^{27,30} Since in reality, both the pre-exponential factor and the activation energy for a given reaction channel determine the overall reaction probability, only when product yields are measured can we say which reaction path is the preferred mode for H-abstraction. Such measurements have been performed for H-atom, O-atom and OH radical reactions with alkanes. For the series: CH_4 , CH_3CH_3 , $(CH_3)_2CH_2$ and $(CH_3)_3CH$, the total observed rate coefficients increase from left to right for all three reactants.^{27,31-33} It has further been shown that for $(CH_3)_2CH_2$ and $(CH_3)_3CH$, there is preferential removal of the secondary and tertiary hydrogens by the three transient species. The secondary and tertiary C-H bonds in these molecules are known to be weaker than the C-H bonds on the methyl moiety. Hence in these reactions there is a strong correlation between the bond strength and the observed reaction rate at the bond site of interest.

The negative temperature dependence and the lack of a pressure dependence we observe for $O(^3P) + N_2H_4$ reaction is not inconsistent with a mechanism involving the formation of an adduct as was the case for the corresponding OH reaction. Subsequent

decomposition of this, in principle, may lead to a variety of products;



We have already assessed the importance of the forth channel to be minor by direct laser-induced fluorescence detection of the OH.⁶ Currently we are in the process of quantifying NH, NH₂ and HNO by this technique also.¹⁷ Previous mass-spectrometric ion-current yield measurements^{21,23} at m/e of 31 for N₂H₃ (or HNO), at 30 for N₂H₂, at 18 for H₂O, and at 17 for OH (or NH₃) qualitatively confirm our OH observations, and suggest channel five to be the dominate process. Direct ir-observations of N₂H₂ are desirable to confirm this.¹⁷ Also, ab initio studies on the energy and geometrical profiles of possible reaction intermediates and transition-states for this reaction would help in the proper elucidation of the nature of the reaction mechanism.

Assuming an average [O(³P)] of 1 x 10¹² molec cm⁻³ at LEO altitudes, the estimated thermospheric lifetimes are ~ 0.6 s, ~ 47 ms, and ~ 78 ms, respectively for N₂H₄, CH₃NHNH₂ and (CH₃)₂NNH₂ at a typical temperature of 800 K. Chemical lifetimes in the immediate vicinity of the spacecraft exhaust may be even shorter because of higher O(³P) concentrations and due to reactions with other effluents. By analogy, we might expect the N₂H₂ molecule to also react rapidly with the O(³P), preferentially via the removal of two H-atoms to give (N₂(A) + H₂O) as the main products. The subsequent energy transfer reactions of the metastable nitrogen, N₂(A), would then provide a mechanism to produce electronically excited radicals such as OH(A²Σ⁺), NH(A³Π), NH₂($\tilde{\text{A}}^2\text{A}_1$), and NO(A²Σ⁺) which have previously been observed in rocket plume environments. The yield of N₂H₂ in channel 5 and from the subsequent oxidation of N₂H₃ from channel 4 will govern the maximum uv-radiance one can expect from the above scheme. To understand the relative importance of uv-excitation by this method compared to that from other sources of N₂(A), or due to alternate precursor energy transfer reactions like those of CO(a),

or that resulting from direct chemiluminescent reactions involving carbonaceous species, a detailed knowledge of the chemical and physical composition of the alkylated diamine rocket plumes will be required.

ACKNOWLEDGMENT

Funding for this work was provided by the Air Force Office for Scientific Research, and carried out at the Air Force Research Laboratory, Edwards AFB, CA, under Contract No. F04611-93-C-0005.

REFERENCES

1. L. S. Bernstein, J. W. Duff, D. S. Frankel, M. E. Gersh, C. E. Kolb, R. B. Lyons, D. C. Robertson, J. B. Elgin, A. McIntyre, N. B. Wheeler, R. E. Huffman, D. E. Frankel, F. J. LeBlanc, V. C. Baisley, and J. C. Larrabee, "MSMP TEM-2 Infrared and Ultraviolet Radiation Data Analysis", **ARI-RN-225**, Aerodyne Research, Inc., January 1981.
2. D. E. Paulsen, J. W. Duff, R. B. Lyons, M. E. Gersh, C. E. Kolb, D. E. Frankel, J. B. Elgin, A. McIntyre, R. Cormier, N. B. Wheeler, W. B. Miller, and R. E. Huffman, "MSMP TEM-3 Infrared and Ultraviolet Radiation Data Analysis", **ARI-RN-227**, Aerodyne Research, Inc., March 1984.
3. O. J. Orient, K. E. Martus, A. Chutjian, and E. Murad, "Optical Emission Generated by Collisions of 5 eV O(³P) Atoms With Surface-Adsorbed Hydrazine", *J. Chem. Phys.*, **97**, 4111 (1992).
4. O. J. Orient, A. Chutjian, and E. Murad, "Observation of CH A→X, CN B→X, and NH A→X Emissions in Gas-Phase Collisions of Fast O(³P) Atoms With Hydrazines", *J. Chem. Phys.*, **101**, 8297 (1994).
5. K. H. Becker and K. D. Bayes, "A Study of the Chemiluminescence From Oxygen Atom-Hydrazine Flames", *J. Phys. Chem.*, **71**, 371 (1967).
6. G. L. Vaghjiani, "Discharge Flow-tube Studies of O(³P) + N₂H₄ Reaction: The Rate Coefficient values over the Temperature Range 252-423 K and the OH(X²Π) Product Yield at 298K", *J. Chem. Phys.*, **104**, 5479 (1996).

7. G. L. Vaghjiani, "UV Absorption Cross Sections for N_2H_4 Vapor Between 191-291 nm and $H(2S)$ Quantum Yield in 248-nm Photodissociation at 296 K", J. Chem. Phys., **98**, 2123 (1993).
8. G. L. Vaghjiani, "UV Absorption Cross Sections, Laser Photodissociation Product Quantum Yields, and the Reaction of H-atoms With Methylhydrazines at 298 K", J. Phys. Chem., **101**, 4167 (1997).
9. C. J. Howard, "Kinetic Measurements Using Flow Tubes", J. Phys. Chem. **83**, 3, (1979).
10. F. Kaufman, "The Air Afterglow and its use in the Study of Some Reactions of Atomic Oxygen", Proc. R. Soc. London Ser. A **247**, 123 (1958), and "Reactions of Oxygen Atoms", Prog. React. Kinet. **1**, 3 (1961).
11. G. L. Vaghjiani, "Laser Potolysis Studies of Hydrazine Vapor: 193 and 222-nm H-atom Primary Quantum Yields at 296 K, and the Kinetics of $H + N_2H_4$ Reaction Over the Temperature Range 222-657 K", Int. J. Chem. Kinet., **27**, 777 (1995).
12. G. L. Vaghjiani and A. R. Ravishankara, "The Rate Coefficient for the Reaction of $O(^3P)$ With CH_3OOH at 297 K", Int. J. Chem. Kinet., **22**, 351 (1990).
13. G. L. Vaghjiani and A. R. Ravishankara, "Kinetics and Mechanism of OH Reaction With CH_3OOH ", J. Phys. Chem., **93**, 1948 (1989).
14. J. D. Hirschfelder, C. F. Curtiss, and R. B. Bird, *Molecular Theory of Gases and Liquids* (Wiley, New York, 1954).
15. G. W. Harris, R. Atkinson, and J. N. Pitts, Jr., "Kinetics of the Reactions of the OH Radical With Hydrazine and Methylhydrazine", J. Phys. Chem., **83**, 2557 (1979).
16. W. Hack, K. Hoyer mann, and H. Gg. Wagner, "Reaktionen des Hydroxylradikals mit Ammoniak und Hydrazin in der Gasphase", Ber. Bunsenges. Phys. Chem., **78**, 386 (1976).
17. G. L. Vaghjiani, "Work in Progress", J. Phys. Chem., **to be submitted** (1998).
18. D. A. Armstrong, D. Yu, and A. Rauk, "Gas Phase and Aqueous Thermochemistry of Hydrazine and Related Radicals and the Energy Profiles of Reactions With H and OH: An ab Initio Study", J. Phys. Chem., **101**, 4761 (1997).
19. See for example, Y. Chen, A. Rauk, and E. T. Roux, "On the Question of Negative Activation Energies: Absolute Rate Constants by RRKM and G1 Theory for $CH_3 + HX \rightarrow CH_4 + X$ ($X = Cl, Br$) Reactions", J. Phys. Chem., **95**, 9900 (1991), and R. J. Berry and P. Marshall, "A Computational Study of the Reaction Kinetics of Methyl Radicals With Trifluorohalomethanes", Int. J. Chem. Kinet., **30**, 179 (1998).
20. E. C. Tuazon, W. O. L. Carter, A. M. Winer, and J. N. Pitts, Jr., "Reactions of Hydrazine With Ozone Under Simulated Atmospheric Conditions", J. Phys. Chem., **15**, 823 (1981).
21. M. Gehring, K. Hoyer mann, H. Gg. Wagner, and J. Wolfrum, "Die Reaktion von Atomarem Sauerstoff mit Hydrazin", Ber. Bunsenges. Phys. Chem., **73**, 956 (1969), and M. Gehring, K. Hoyer mann, H. Schacke, and J. Wolfrum, "Direct Studies of Some Elementary Steps for the Formation and Destruction of Nitric Oxide in the H-N-O System", Symp. (Int.) Combust. Proc. **14**, 99 (1972).
22. V. I. Lang, "Rate Constants for Reactions of Hydrazine Fuels With $O(^3P)$ ", J. Phys. Chem., **96**, 3047 (1992).
23. S. N. Foner and R. L. Hudson, "Mass Spectrometry of Very Fast Reactions: Identification of Free Radicals and Unstable Molecules Formed in Atom-Molecule Reactions", J. Chem. Phys., **49**, 3724 (1968), and S. N. Foner and R. L. Hudson, "Mass Spectrometric Studies of Atom-Molecule Reactions Using High-Intensity Crossed Molecular Beams", J. Chem. Phys., **53**, 4377 (1970).
24. C. F. Melius, *BAC-MP4 Heats of Formation and Free Energies* (Sandia National Laboratory, Livermore, 1993).
25. S. W. Benson, *Thermochemical Kinetics* (Wiley, New York, 1976).
26. M. W. Chase, Jr., C. A. Davies, J. R. Downey, Jr., D. J. Frurip, R. A. McDonald, and A. N. Syverud,

"JANAF Thermochemical Tables, Third Edition", J. Phys. Chem. Ref. Data, **14**, Suppl. 1 (1985).

27. F. Westley, D. H. Frizzell, J. T. Herron, R. F. Hampton, and W. G. Mallard, *Nist Chemical Kinetics Database* (NIST Standard Reference Database 17, Gaithersburg, 1994), and references therein.

28. R. Atkinson and J. N. Pitts, Jr., "Kinetics of the Reactions of $O(^3P)$ Atoms With the Amines CH_3NH_2 , $C_2H_5NH_2$, $(CH_3)_2NH$, and $(CH_3)_3N$ Over the Temperature Range 298-440 K", J. Chem. Phys., **68**, 911 (1978).

29. D. F. McMillen and D. M. Golden, "Hydrocarbon Bond Dissociation Energies", Ann. Rev. Phys. Chem., **33**, 493 (1982).

30. R. Atkinson, R. A. Perry, and J. N. Pitts, Jr., "Rate Constants for the Reactions of the OH Radical With $(CH_3)_2NH$, $(CH_3)_3N$, and $C_2H_5NH_2$ Over the Temperature Range 298-426K", J. Chem. Phys., **68**, 1850 (1978).

31. W. Tsang, "Chemical Kinetic Data Base for Combustion Chemistry Part 4. Isobutane", J. Phys. Chem. Ref. Data, **19**, 1 (1990), and references therein.

32. W. Tsang, "Chemical Kinetic Data Base for Combustion Chemistry Part 3. Propane", J. Phys. Chem. Ref. Data, **17**, 887 (1988), and references therein.

33. R. Atkinson, "Kinetics and Mechanisms of the Gas-Phase Reactions of the Hydroxyl Radical With Organic Compounds", J. Phys. Chem. Ref. Data, Monograph **1** (1989), and references therein.